Dynamic Collimator Rotation Treatment Plan Optimization for O-Ring Treatment Systems

Michael K Fix, Werner Volken, Daniel Frei, Silvan Mueller, Gian Guyer, Daniel Schmidhalter, and Peter Manser

Division of Medical Radiation Physics and Department of Radiation Oncology, Inselspital,
Bern University Hospital, and University of Bern, Bern, Switzerland

Abstract In intensity modulated radiotherapy (IMRT) and volumetric modulated arc therapy (VMAT) static collimator angles are used per field or arc. While dynamic collimator rotation during beam on was investigated for C-arm linear accelerators, this was not investigated for O-ring ETHOS/Halcyon treatment systems. This work aims in the development of an optimization framework for treatment plans with dynamic collimator rotation during beam on for ETHOS/Halcyon systems. A previously developed in-house hybrid direct aperture optimization algorithm was first extended with a Monte Carlo (MC) model of the ETHOS/Halcyon treatment head including the double stack multi leaf collimator to calculate MC beamlet dose distributions and second with options for dynamic collimator rotation optimization for IMRT and VMAT. The framework was tested for a clinically motivated case showing improved dose sparing for organs at risk using dynamic collimator angle rotation compared with static collimator angle treatment plans, while the target coverage was the same.

1 Introduction

Currently, intensity modulated radiotherapy (IMRT) and volumetric modulated arc therapy (VMAT) are well-established state-of-the-art treatment techniques in radiotherapy [1,2]. More recently, there is an increasing interest in exploiting additional degrees of freedom in radiotherapy treatment planning to further improve treatment plan quality [3]. There is a variety of these techniques investigated ranging from using multiple arcs at different static table angles to dynamic trajectory radiotherapy (DTRT) using simultaneous dynamic gantry, table and collimator rotation during beam on leading to promising results in terms of treatment plan improvements [3–6]. While dynamic collimator rotation as a degree of freedom for dynamic collimator radiotherapy was investigated for C-arm linear accelerators, this was not yet investigated for O-ring ETHOS or Halcyon treatment systems.

Previously, we developed an in-house optimization framework within a treatment planning process to generate deliverable DTRT treatment plans for C-arm linear accelerators [7]. This framework consists of a hybrid direct aperture optimization (HDAO) algorithm, which combines a column generation algorithm with simulated annealing and is based on Monte Carlo (MC) generated beamlet dose distributions used to determine the aperture shape along with the Monitor Unit (MU) weight. However, this HDAO cannot be directly applied to ETHOS/Halcyon treatment systems, as those system consists of a different beam defining system including a unique double stack multi leaf collimator (MLC).

The aim of this work is the development of an optimization framework for VMAT and IMRT treatment plans with dynamic collimator rotation for ETHOS/Halcyon treatment systems to improve treatment plan quality compared to plans with static collimator rotation angels. For this purpose, first a MC model for an ETHOS/Halcyon treatment system was implemented and commissioned for an ETHOS unit to be used to generate MC beamlet dose distributions for the HDAO. Second, the HDAO algorithm was extended in order to handle the double stack MLC and the dynamic collimator rotation in the optimization. Finally, the developed framework was tested for a clinically motivated head and neck case.

2 Materials and Methods

In a first part of this work, an MC model of the beam defining system for an ETHOS/Halcyon treatment system consisting of the target, the primary collimator, the monitor chamber, the secondary collimator, the double-stack MLC and the leaf box cover as illustrated in Figure 1 was implemented into our in-house developed Swiss Monte Carlo Plan (SMCP) [8] following the information provided by the vendor (Varian, a Siemens Healthineers Company).

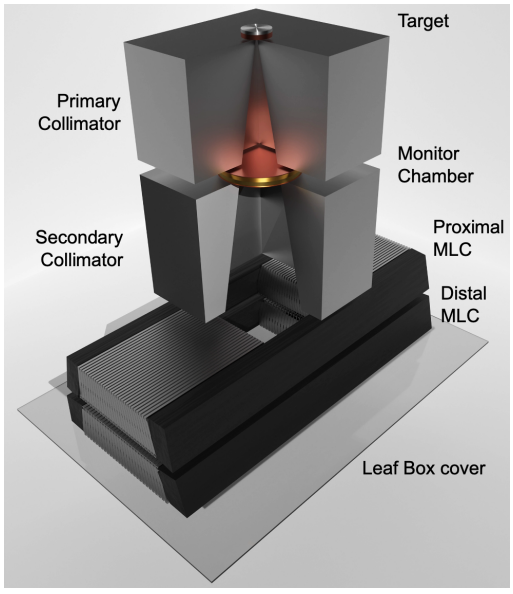

Figure 1: Illustration of the beam defining components for the ETHOS/Halcyon treatment system as implemented in the SMCP.

For the commissioning of the model, the energy and the lateral fluence distribution of the initial electron beam impinging on the target were tuned to match measured dose distributions. For this purpose, depth dose curves and lateral dose profiles in five depths ranging from 1.3 cm to 15 cm

were measured for square MLC shaped field sizes ranging from 1 x 1 cm^2 to 28 x 28 cm^2 at a source to surface distance (SSD) of 100 cm in units of cGy/MU on an ETHOS treatment system. For the validation the analogous set of dose distributions at an SSD of 90 cm were measured and compared with the corresponding calculated dose distributions using the commissioned MC model.

The implemented MC model was used in our HDAO algorithm. However, this HDAO so far is not able to handle the double stack MLC of an ETHOS/Halcyon system. This double stack ETHOS/Halcyon MLC consists of a proximal part with 29 leaf pairs and a distal part with 28 leaf pairs. In the following these are referred to as the physical MLC leaves. The width for each individual physical MLC leaf is 1 cm in the isocenter plane. The positions of the physical 57 MLC leaf pairs can be described by a set of 2 x 57 numbers. In general, the combination of two field shapes individually defined by the proximal and the distal MLC parts can be described with 56 so-called pseudo-MLC leaf pairs with a width of 0.5 cm in the isocenter plane, i.e. any combination of proximal and distal MLC leaf patterns (physical aperture) can be represented unambiguously by a pseudo leaf pair pattern (pseudo aperture). An example of such a conversion from a physical to a pseudo aperture is illustrated in Figure 2.

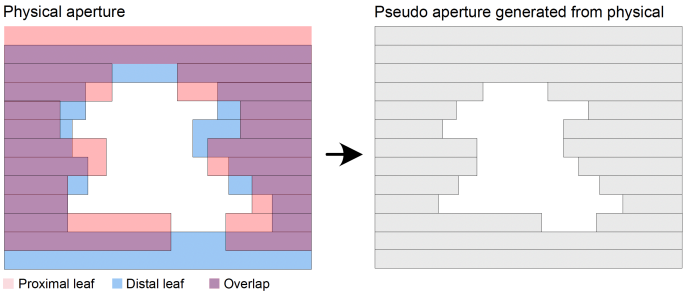

Figure 2: Illustration of the conversion from physical leaf positions to pseudo leaf positions. The graphics on the left shows the combination of a proximal and a distal MLC leaf pattern (physical aperture), while the graphics on the right-hand side shows its representation using the pseudo-MLC leaves (pseudo aperture).

Consequently, 56 x 56 beamlets with a size of 0.5 x 0.5 cm^2 each were generated using the commissioned MC model and serve as a base for the beamlet dose calculation resulting in the dose influence matrix applied during optimization. During the HDAO, the optimization algorithm keeps track of two sets of numbers representing the physical aperture (2 x 57 numbers) as well as the pseudo aperture (2 x 56 numbers). Both sets are always synchronized to guarantee that beamlet selection based on pseudo apertures is in compliance with the corresponding physical apertures.

In addition, the HDAO was extended to include the dynamic collimator rotation angle in the treatment planning process with different approaches for IMRT and VMAT.

In the case of IMRT, a set of 12 equi-angular beam directions are provided as input for the HDAO. This setup corresponds to our standard IMRT setup template of the ETHOS planning system. The number of apertures was limited to a total of 100, based on previous investigations with the HDAO. Next, beamlet dose distributions per beam directions were calculated for different collimator angles. This was done for a set of discrete collimator angles {-80°, -60°, -40°, -20, 0°, 20°, 40°, 60°, 80°} referred to as *'optimized collimator angle'* method (*oca*) leading to an increased search space of promising apertures for each beam direction. This newly developed method was compared with using a static static collimator angle of 10° for all apertures and all beam directions referred to as *'static collimator angle'* method (*sca*).

In the case of VMAT, the *oca* method would allow large collimator angle rotation changes between adjacent control points resulting in excessive collimator movement. In addition, this would also need an enormous amount of beamlet dose calculations. Thus, an approach was implemented in which the gantry-collimator path is predefined and provided as input to the HDAO. For this purpose, we implemented a '*predefined collimator angle*' method (*pca*). In this *pca* method a A* path finding algorithm is applied with a maximum gradient of 4°/5° (collimator/gantry) to a gantry-collimator whitespace area map to find the gantry-collimator path that maximally reduce the whitespace area. For this map, first the area between the PTV structure is extended by an isotropic margin of 0.5 cm. Then, the conformal MLC opening (whitespace area) is determined as a function of the gantry and collimator rotation angle settings leading to a two-dimensional gantry-collimator map. The resulting path was then passed to the HDAO for optimization.

Finally, this developed HDAO framework was tested for a clinically motived head and neck case and treatment plans for a 12 field IMRT and a two full arc VMAT technique with and without dynamic collimator rotation were generated. For the optimization the objectives for the intensity modulation optimization were based on those used for the clinically delivered treatment plan. The optimization utilizing a static or a dynamic collimator rotation used the same set and values for the objectives and priorities as well as the same objective function. For all these comparisons the normalization was such that 95% von the PTV ($D_{95\%}$) receives the prescribed dose. Resulting treatment plan qualities using either a dynamic collimator angle or a static collimator angle were compared by means of the dose distributions and dose volume histogram parameters.

3 Results

An MC model of the ETHOS/Halcyon radiotherapy beam was successfully implemented in the SMCP. The commissioned MC model for an ETHOS treatment system agreed in general within 1% (global) or 1 mm for all depth dose curves and lateral dose profiles in units of cGy/MU for

all square field sizes considered in the validation. Figure 3 shows some exemplary results of this validation.

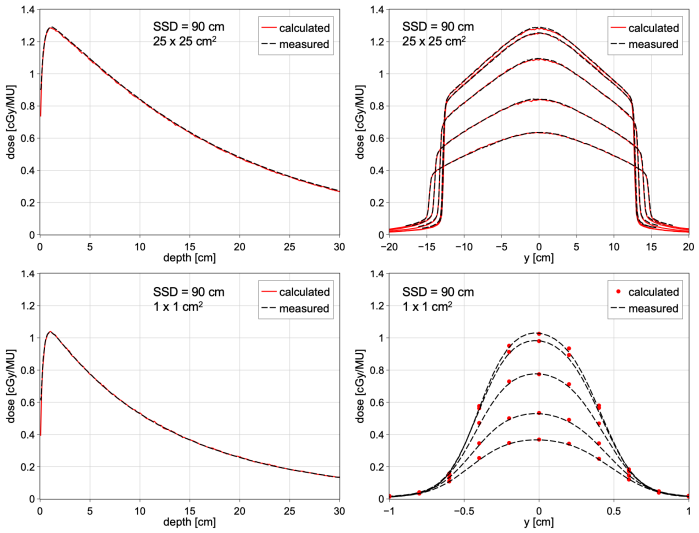

Figure 3: Absolute dose comparisons of calculated dose distributions with the corresponding measured dose distributions in homogeneous water at an SSD = 90 cm for field sizes of 25 x 25 cm² (top row) and 1 x 1 cm² (bottom row) using the commissioned MC model. Depth dose curves and lateral dose profiles in five depths (1.3 cm, 2 cm, 5 cm, 10 cm, 15 cm) of water in y-direction are shown for each field size. The agreement is generally within 1% or 1 mm.

In Figure 4 the results for the clinically motivated head and neck case are presented utilizing the 12 field IMRT technique.

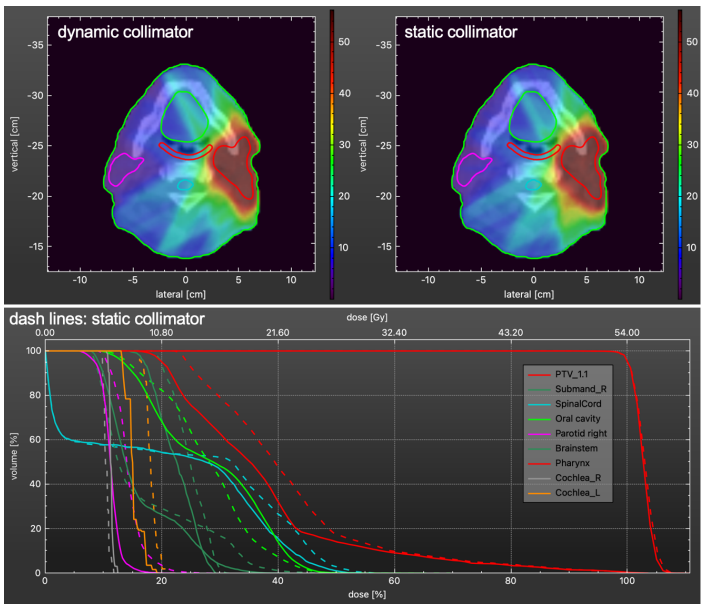

Figure 4: Dose distributions and DVH comparisons for IMRT treatment plans using either the dynamic collimator angle approach or the static collimator angle approach for a clinically motivated head and neck case. For this comparison the 'optimized collimator angle' (oca) method was used to determine the collimator angle for each individual aperture of the beam directions.

Both treatment plans result in a very similar target coverage, while improved dose distributions were achieved for the treatment plan with dynamic collimator rotation when compared with the treatment plan using a static collimator rotation of 10° for all apertures.

The results for the two-arc VMAT treatment plans are illustrated in Figure 5. Again, the target coverage was very similar for the two treatment techniques. For the plan using a static collimator rotation angle per arc the values of 9° and 29° were used (one value per arc). The OAR sparing improvements for the treatment plan including the dynamic collimator rotation vs. the treatment plan using static collimator angles was less pronounced for the VMAT technique when compared with the IMRT delivery modality. The dose volume histogram parameters for the comparisons are summarized in Table 1.

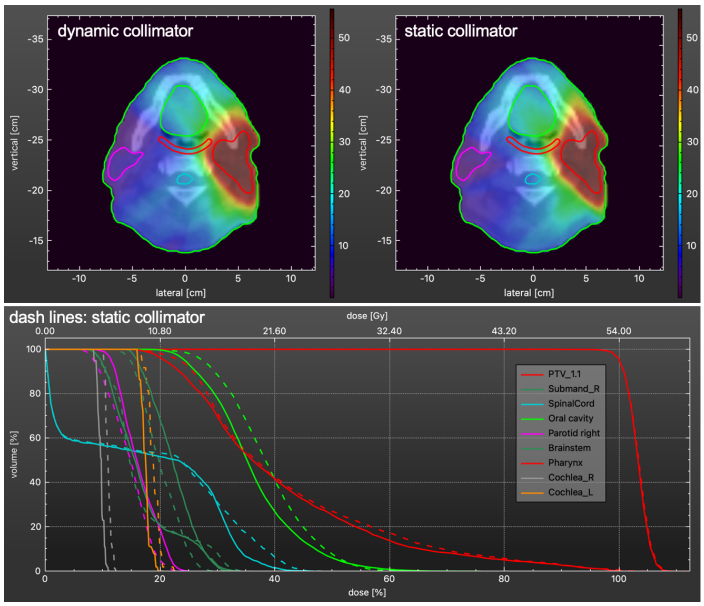

Figure 5: Dose distributions and DVH comparisons for the two-arcs VMAT treatment plans using either the dynamic collimator angle approach or the static collimator angle approach for the clinically motivated head and neck case already shown in Figure 4. For this comparison the predefined collimator angle (pca) method was utilized, where the A algorithm was used to determine the collimator rotation angle as a function of the gantry angle.*

Table 1: Comparison of dosimetric parameters for the dose distributions of treatment plans without (IMRT, VMAT) and with ($IMRT_{dyn}$, $VMAT_{dyn}$) dynamic collimator rotation for the clinically motivated head and neck case shown in Figures 4 and 5. Superior values are highlighted in bold (HI = homogeneity index; CI = conformity index).

PTV	**IMRT**	**$IMRT_{dyn}$**	**VMAT**	**$VMAT_{dyn}$**
$D_{98\%}$ [Gy]	53.6	53.6	53.5	53.5
$D_{2\%}$ [Gy]	57.3	**57.1**	57.8	**57.7**
HI	0.070	**0.065**	0.082	**0.079**
CI	0.695	**0.714**	0.718	**0.721**
Submadible right				
D_{mean} [Gy]	13.4	**12.1**	**10.8**	12.0
$D_{2\%}$ [Gy]	16.2	**15.5**	**14.5**	16.3
Spinal Cord				
Dmean [Gy]	12.3	**11.3**	9.8	**9.3**
$D_{2\%}$ [Gy]	27.5	**26.2**	23.1	**21.2**
Oral Cavity				
D_{mean} [Gy]	**15.0**	15.2	20.9	**19.5**
$D_{2\%}$ [Gy]	**23.9**	24.4	**29.6**	30.2
Parotid right				
D_{mean} [Gy]	7.7	**6.0**	**7.8**	8.8
$D_{2\%}$ [Gy]	11.4	**8.2**	**11.5**	12.3
Brainstem				
D_{mean} [Gy]	9.2	**8.8**	9.1	**9.0**
$D_{2\%}$ [Gy]	20.6	**17.5**	17.3	**16.2**
Pharynx				
D_{mean} [Gy]	22.6	**20.1**	23.0	**22.3**
$D_{2\%}$ [Gy]	48.0	**47.5**	50.4	**50.1**
Chochlea right				
D_{mean} [Gy]	**5.6**	6.1	5.9	**5.2**
$D_{2\%}$ [Gy]	**6.3**	6.7	6.5	**5.8**
Cochlea left				
D_{mean} [Gy]	9.8	**8.1**	10.1	**9.4**
$D_{2\%}$ [Gy]	10.8	**9.9**	11.0	**10.3**

4 Discussion

We have successfully implemented and commissioned an MC model of the beam defining components of an ETHOS treatment system. The validated MC model is now available within the SMCP for accurate dose calculation. The level of accuracy is similar to the results shown by Laakkonen et al. [9]. In addition, this model was successfully integrated in our in-house optimization framework, which was extended to allow optimization for an ETHOS/Halcyon system including the double stack MLC as well as for dynamic collimator angle rotation.

While the results of this work focused on an ETHOS treatment system, the developed framework is also suitable for Halcyon treatment systems, as the beam defining system components are the same. However, the MC model would have to be commissioned for the different systems.

The currently used clinical ETHOS/Halcyon treatment systems do not allow dynamic collimator rotation during beam on for VMAT. However, the generated treatment plans take into account all mechanical and dosimetric influencing parameters and contributions in the final dose calculation and consequently such VMAT treatment plans can be considered as potentially deliverable treatment plans. Although in this study only one clinically motivated case was investigated, the results demonstrate potential for dynamic collimator rotation treatment plans to improve OAR sparing when compared with treatment plans using static collimator rotation angles. However, a larger number of clinically motivated cases has to be investigated to determine the potential dosimetric benefit of dynamic collimator rotation radiotherapy for ETHOS/Halcyon treatment systems.

5 Conclusion

We have successfully implemented an optimization framework for dynamic collimator rotation optimization for ETHOS/Halcyon treatment systems based on MC generated beamlet dose distributions. The results suggest potential benefits for OAR sparing when dynamic collimator rotation is applied. The framework can now be used to investigate the potential benefit of dynamic collimator radiotherapy for a larger patient cohort.

Acknowledgements

This work was supported by Varian, a Siemens Healthineers Company. Dose calculations and optimizations were performed on UBELIX (www.id.unibe.ch/hpc), the high-performance cluster at the University of Bern.

References

[1] Yu CX. Intensity-modulated arc therapy with dynamic multileaf collimation: an alternative to tomotherapy. Phys Med Biol 1995;40:1435–49. https://doi.org/10.1088/0031-9155/40/9/004.

[2] Otto K. Volumetric modulated arc therapy: IMRT in a single gantry arc. Med Phys 2008;35:310–7. https://doi.org/10.1118/1.2818738.

[3] Smyth G, Evans PM, Bamber JC, Bedford JL. Recent developments in non-coplanar radiotherapy. Br J Radiol 2019;92:20180908. https://doi.org/10.1259/bjr.20180908.

[4] Fix MK, Frei D, Volken W, Terribilini D, Mueller S, Elicin O, et al. Part 1: Optimization and evaluation of dynamic trajectory radiotherapy. Med Phys 2018. https://doi.org/10.1002/mp.13086.

[5] Bertholet J, Mackeprang P-H, Mueller S, Guyer G, Loebner HA, Wyss Y, et al. Organ-at-risk sparing with dynamic trajectory radiotherapy for head and neck cancer: comparison with volumetric arc therapy on a publicly available library of cases. Radiat Oncol 2022;17:122. https://doi.org/10.1186/s13014-022-02092-5.

[6] Guyer G, Mueller S, Koechli C, Frei D, Volken W, Bertholet J, et al. Enabling non-isocentric dynamic trajectory radiotherapy by integration of dynamic table translations. Phys Med Biol 2022;67:175003. https://doi.org/10.1088/1361-6560/ac840d.

[7] Mueller S, Guyer G, Risse T, Tessarini S, Aebersold DM, Stampanoni MFM, et al. A hybrid column generation and simulated annealing algorithm for direct aperture optimization. Phys Med Biol 2022;67. https://doi.org/10.1088/1361-6560/ac58db.

[8] Fix MK, Manser P, Frei D, Volken W, Mini R, Born EJ. An efficient framework for photon Monte Carlo treatment planning. Phys Med Biol 2007;52:N425-437. https://doi.org/10.1088/0031-9155/52/19/N01.

[9] Laakkonen L, Lehtomäki J, Cahill A, Constantin M, Kulmala A, Harju A. Monte Carlo modeling of Halcyon and Ethos radiotherapy beam using CAD geometry: validation and IAEA-compliant phase space. Phys Med Biol 2023;68:044002. https://doi.org/10.1088/1361-6560/acb4d9.